

THE BULGE RADIAL VELOCITY ASSAY (BRAVA): TECHNIQUES AND A ROTATION CURVE

R. MICHAEL RICH, DAVID B. REITZEL, AND CHRISTIAN D. HOWARD¹
 Department of Physics and Astronomy, UCLA, Los Angeles, CA 90095-1547

HONGSHENG ZHAO

SUPA, School of Physics and Astronomy, University of St Andrews, KY16 9SS, UK
Submitted to the Astrophysical Journal Letters

ABSTRACT

We are undertaking a large scale radial velocity survey of the Galactic bulge which uses M giant stars selected from the 2MASS catalog as targets for the CTIO 4m Hydra multi-object spectrograph. The aim of this survey is to test dynamical models of the bulge and to quantify the importance, if any, of cold stellar streams in the bulge and its vicinity. Here we report on the kinematics of a strip of fields at $-10^\circ < l < +10^\circ$ and $b = -4^\circ$. We construct a longitude-velocity plot for the bulge stars and the model data, and find that contrary to previous studies, the bulge does not rotate as a solid body; from $-5^\circ < l < +5^\circ$ the rotation curve has a slope of roughly $100 \text{ km s}^{-1} \text{ kpc}^{-1}$ and flattens considerably at greater l and reaches a maximum rotation of 45 km s^{-1} . This rotation is slower than that predicted by the dynamical model of Zhao (1996) and slower than found for planetary nebulae (Beaulieu et al. 2000). Our velocity dispersion profile is in good agreement with the Zhao model, but the slower rotation field suggests that the current model requires the inclusion of retrograde orbits. The high precision of our radial velocities ($\sim 3 \text{ km s}^{-1}$) yields an unexpected result: hints of cold kinematic features are seen in a number of the line of sight velocity distributions.

Subject headings: Galaxy: bulge – Galaxy: kinematics and dynamics – Stars: late-type – stars:kinematics – techniques: radial velocities

1. INTRODUCTION

The COBE 2 μm image of the bulge (Dwek et al. 1995) shows evidence for a bar-like structure that also appears in star counts of red clump stars (Stanek et al. 1997). The anomalously high optical depth of the bulge to micro-lensing (Alcock et al. 2000) can be understood only if there is a bar whose major axis extends roughly toward the Sun, thus raising the rate of star-star events (Han & Gould 2003). Theoretical models of the bulge initially followed axisymmetric models (Kent 1992) but have graduated to self-consistent rapidly rotating bars (Zhao 1996; Binney, Gerhard, & Spergel 1997) ready for a new generation of observational data to constrain them.

Study of the kinematics of the bulge is complicated by the large and variable foreground extinction, the presence of a contaminating disk population extending from the foreground well into the Galactic Center, and source confusion arising from the high density of stars. Positional measurements from wide field Schmidt plates are therefore impossible, where source confusion makes any astrometric exercise daunting.

M giants, while faint in the traditional optical bandpasses due to their cool temperatures and TiO bands, are bright in the I band ($13 < I < 11$) and easy targets for spectroscopy if positions can be obtained. They further have the advantage of being ubiquitous throughout the bulge and are luminous enough to be studied even in fields with substantial extinction. Finally, the short lifetimes of AGB stars and luminous giants limit their numbers enough that source confusion is not an issue.

Mould (1983) was the first to measure the velocity dispersion of the bulge in Baade's Window, based on the M giant sample of Blanco, McCarthy, & Blanco (1984) that was first classified from low dispersion slitless spectra. Multi-fiber spectroscopy of this sample (Sharples, Walker, & Cropper 1990) subsequently harvested roughly 250 bulge giant velocities. Despite numerous investigations of the dynamics of stars in the direction of Baade's Window (Mould 1983; Rich 1990; Sharples, Walker, & Cropper 1990; Sadler, Rich, & Terndrup 1996) and in other bulge fields (Tyson & Rich 1991; Minniti et al. 1992; Minniti 1996; Blum et al. 1994, 1995) there has been, up to now, no large scale survey of the dynamics of the stellar population in the bulge. Beaulieu et al. (2000) survey the planetary nebula population; both the rarity of PNe (due to their brief lifetimes), the problem of disk or bulge membership, and the considerable distance uncertainty make PNe a problematic population; We believe a well selected sample of M giants is likely the best probe of the bulge/bar population.

Frogel & Whitford (1987) showed that the M giant luminosity function is consistent with an old population roughly the age of the halo and globular clusters. The first detailed abundance analysis of M giants (Rich & Origlia 2005) finds an abundance range similar to that of the K giants (McWilliam & Rich 1994; Fulbright et al. 2006). In principle, the most metal-poor component of the bulge population might not evolve through the M giant phase as the K giant

¹ Visiting Astronomers, Cerro Tololo Inter-American Observatory. CTIO is operated by AURA, Inc. under contract to the National Science Foundation.

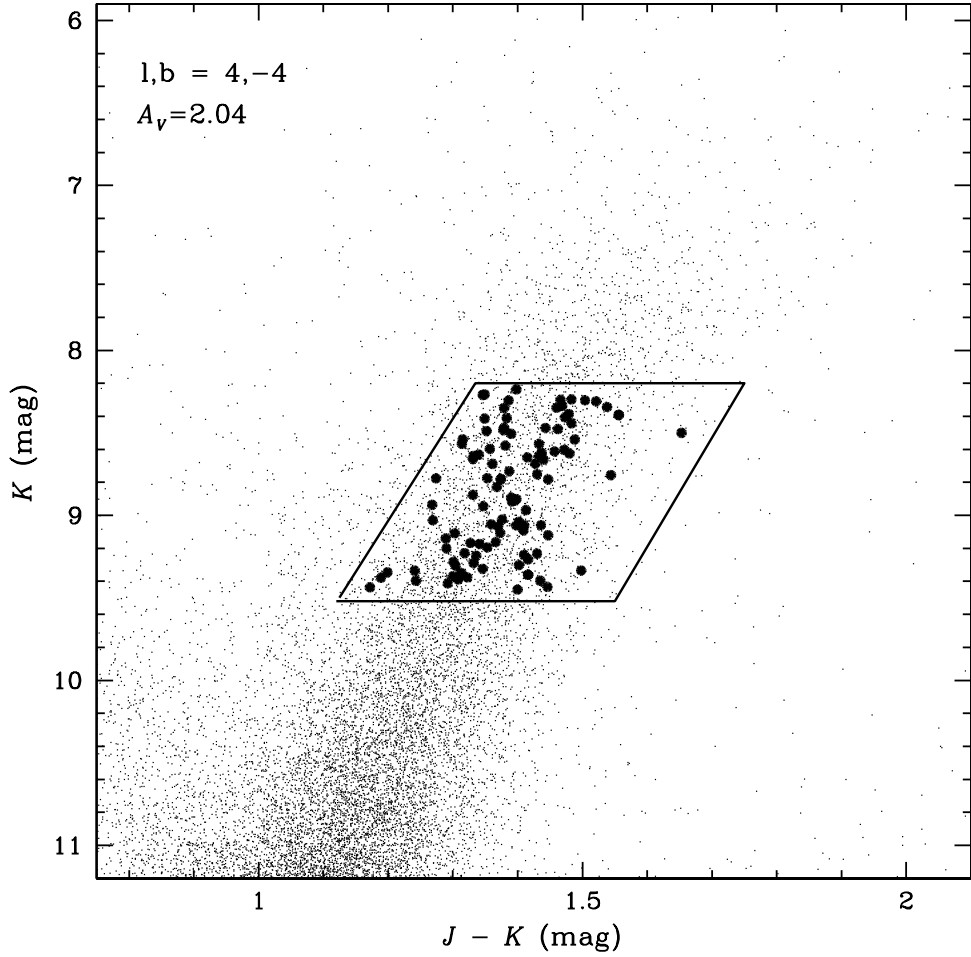


FIG. 1.— Fig. 1: Color-magnitude diagram of 2MASS targets. Filled symbols indicate stars for which we have spectra. The parallelogram indicates our selection region; the blue cutoff rejects many objects that are closer than the bulge, which have lower reddening and are brighter than the red giant branch.

abundance distribution is peaked at slightly sub-solar metallicities, but most of the stars are more metal-rich than 47 Tuc (at -0.7 dex) and are therefore candidates to reach the luminosities and effective temperatures characteristic of the M giants.

The proper motion study of Sumi et al. (2004) addresses a number of fields in the bulge (avoiding high extinction) and eventually, a second epoch of 2MASS imaging would provide proper motions for large numbers of giants. However, the addition of radial velocities and ultimately metal abundances, is needed for a complete dynamical model and the M giant population provides the perfect sample of stars to target.

The dynamical model for the bulge/bar has a number of important implications. Large samples of uniform radial velocity data are still of great value in constraining the bar vs. axisymmetric models, and the nature of the orbit families supporting the bar. Further, the interpretation of the micro-lensing events in the bulge depends on the use of an accurate dynamical model (Han & Gould 2003). The recent discovery of planetary transit host stars in the bulge (Sahu et al. 2006) gives an additional incentive to improve our knowledge of the bulge/bar model.

With the availability of the Two Micron All-Sky Survey 2MASS (Skrutskie et al. 2006) we realized that the key ingredients of high precision positions and photometry would finally be available everywhere in the Galactic bulge except near the plane of the Galaxy. At this time, we present ~ 3000 spectra and have obtained a radial velocity precision of ≈ 3 km s^{-1} for our most recent (2006) data.

In the past, radial velocity studies in the bulge have not emphasized high precision, because of the large velocity dispersion and the expectation that the short orbital periods would phase-wrap any cold structures out of existence in well under a Gyr. Yet our precision is sufficient to enable a search for more cold streams analogous to those associated with the Sagittarius dwarf spheroidal galaxy. Surprisingly, we are detecting apparent cold structures in a large number of our fields; the investigation of these unexpected features will be considered in a future paper.

Here we report on the kinematics of stars along a band at $b = -4^\circ$, obtaining a rotation curve and velocity dispersion profile. This article addresses only the 2006 data; a complete presentation of the full dataset is in preparation.

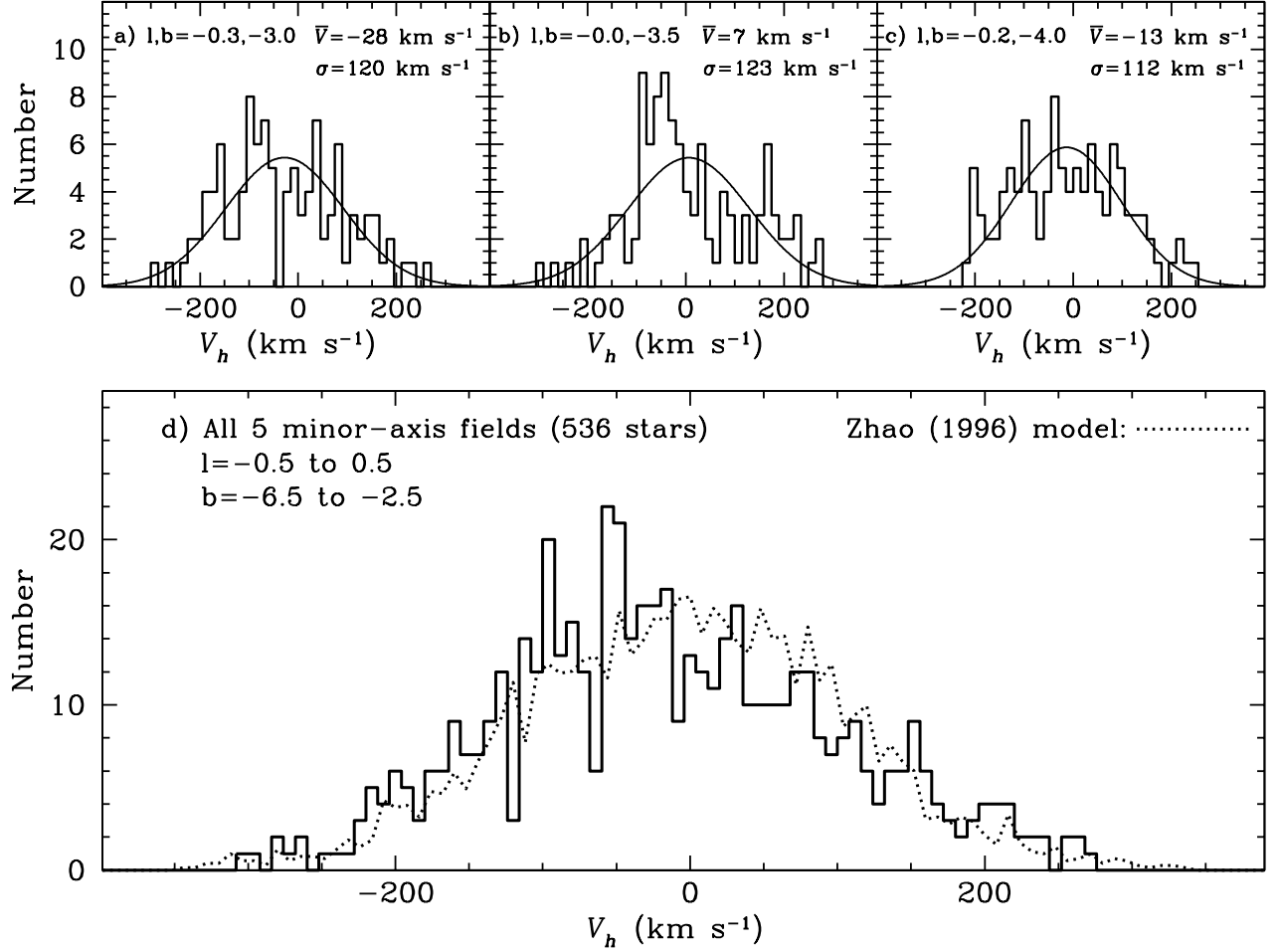


FIG. 2.— Fig. 2a-c.: Velocity dispersion profile of three minor axis fields ranging from $-3^\circ < b < -4^\circ$; note the clumpiness in a and b. The velocity dispersion profile of the sum of these fields is given in Fig 2d. The dotted line is the prediction from the Zhao (1996).

2. OBSERVATIONS

The choice for optical spectroscopy is driven by the availability of multi-object wide field spectroscopy. IR spectroscopy, such as that of Blum et al. (1995), can be used to great effect in the fields of highest reddening but obviously yields far fewer spectra. Here we present a brief sketch of the selection method and analysis; full details will be given in Howard et al. (2007 in prep.).

2.1. Target Selection

We use the survey method of Sharples, Walker, & Cropper (1990) as the model for our program. They found that stars with $I < 11.8$ have a lower velocity dispersion and are likely disk members. When the same field is examined in 2MASS, the K vs $J - K$ CMD shows a clearly defined red giant branch. In the SCW90 field, we find that the magnitude limit of $I < 11.8$ corresponds roughly to $K < 8$. Further, there is a break in the luminosity function at this K magnitude (Frogel & Whitford 1987). While a few bulge AGB members may be present at brighter magnitudes, the bulk of such bright stars will be foreground contaminants. We adopt a range of $9.25 < K < 8$ as the basis for selecting the 2MASS M giants (Figure 1).

A parallelogram shaped selection region is adjusted in color and magnitude according to the reddening of the field as indicated by the reddening map of Schlegel et al. (1998). We find reddening varies greatly ranging from $2.0 < A_V < 5.0$. In fields with high extinction, differential reddening is an issue and we widened the selection region to accommodate the red giant branch as observed (Figure 1).

2.2. Spectroscopy

We use the Hydra multi-fiber spectrograph at the cassegrain focus of the Blanco 4m telescope at Cerro Tololo. We optimize for spectroscopy in the red, taking advantage of the red colors of M giants and employ the KPGLD grating, blazed at 8500\AA giving 0.45\AA pix^{-1} with 2-pixel on-chip binning yielding an effective resolution of 0.88\AA pix^{-1} and a

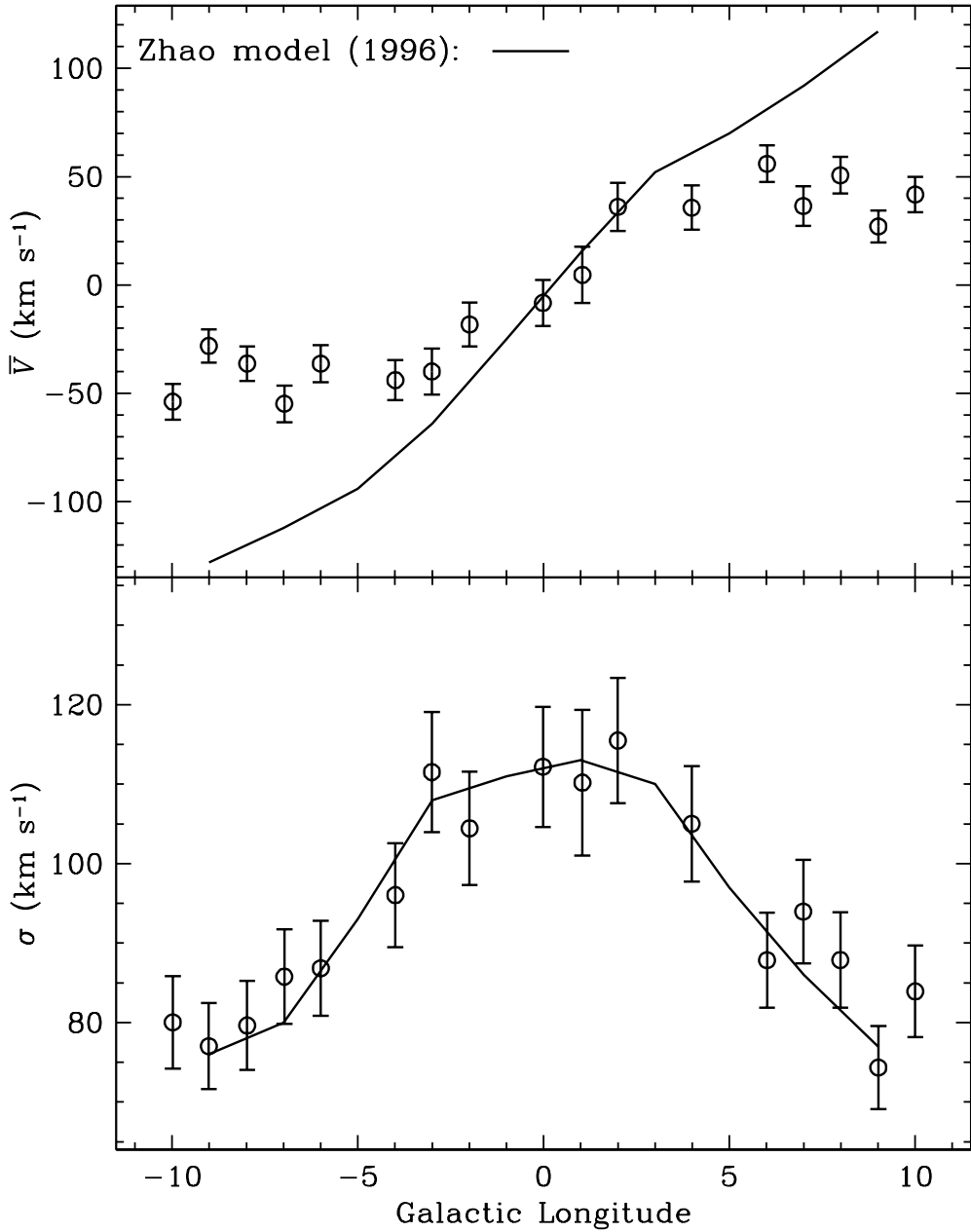


FIG. 3.— Fig. 3a: Rotation curve with predicted dynamics of the Zhao (1996) model indicated by the line. Notice the clear departure from solid body rotation. Fig. 3b: Velocity dispersion with the predictions of Zhao (1996) indicated.

full spectra range of 1800Å. In 2006 we added the 200μm slit plate, giving us an increase in resolution; the loss of light due to using the slit plate is inconsequential to our S/N because the stars are so bright. Our useful spectral range in 2006 was 6891Å to 8714Å; the majority of the stars are so red that the CaII infrared triplet is overwhelmed by the TiO absorption. Our exposures are typically 3 × 600 s but longer exposures were needed when cirrus was present. Each field has on average, 108 successfully exposed M giants and 20 fibers that are used to obtain a sky background spectrum. Flat fielding, sky subtraction, throughput correction, scattered light subtraction, and wavelength calibration for each exposure were all accomplished using the IRAF task dohydra.

The spectra are binned to 34.3 km s⁻¹ pix⁻¹ and normalized. Radial velocities are measured using the fxcor task in IRAF; this requires the spectra to be Fourier filtered exclude features greater than 50 pixels or smaller than 3 pixels in extent. Regions of the spectrum with obvious telluric features were excluded, leaving only 60% of the spectrum usable for cross correlation. Our final cross correlation regions are 7000-7150Å, 7300-7580Å, 7700-8100Å, and 8300-8600Å.

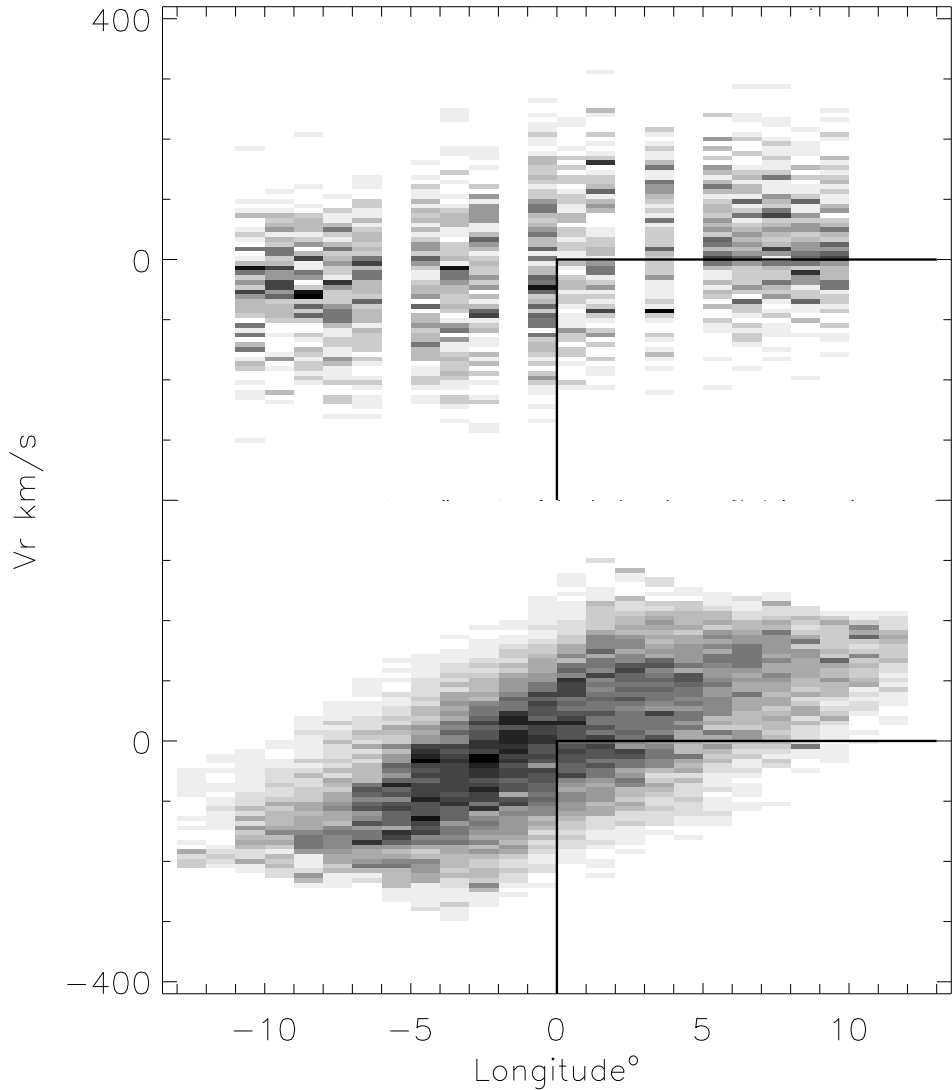


FIG. 4.— Fig. 4: *Upper panel*: longitude-velocity diagram for the data along $b = -4^\circ$, which have been smoothed to 0.5° bins and by 8 km s^{-1} . *Lower Panel*: The same region extracted from the Zhao (1996) model. The solid lines in the lower right indicate the region populated by stochastic orbits in the model. By construction, the model has no retrograde orbits; these would also populate this region and their addition would help bring the model into agreement with the data.

3 standard stars are all used in the cross correlation, with the final velocity for any given star being the average of the 3 derived velocities. The three standards return velocities that agree to within 1.6 km s^{-1} on average, with a standard deviation of 1.4 km s^{-1} in these differences.

In 2006, we measured radial velocities for a total 2294 M giants. Here we report on a set of fields spanning across $b = -4^\circ$. We compare our observed velocities and velocity dispersion with those predicted by the self consistent rotating bulge/bar model of Zhao (1996).

3. MINOR AXIS VELOCITY DISPERSION

In Figure 2 we illustrate the velocity dispersion resulting from the sum of all fields on the minor axis at $b = -2.5^\circ$ to -6.5° as well as three examples of the fields that went into the summed distribution. The best fit Gaussian to the data gives $\sigma = 119 \pm 5 \text{ km s}^{-1}$ with $v_0 = -11 \pm 30 \text{ km s}^{-1}$. A number of peaks are present in this histogram; these are prominent in the contributing histograms (Figure 2a-c). A comparison with the approximately same corresponding region in the Zhao (1996) model is also shown; the agreement is very good, but the velocities in the data appear to be more clumpy than they are in the model. Even more striking peaks are found in some of our other fields; a discussion of the significance of these features will be given in Reitzel et al. 2007 (in prep).

4. THE ROTATION CURVE AND VELOCITY DISPERSION PROFILE

Figure 3a,b shows our rotation curve and velocity dispersion profile compared with that predicted by Zhao (1996); we give the data in Table 1. In contrast with previous studies, we do not observe solid body rotation; after reaching an amplitude of ~ 40 km s $^{-1}$, the rotation curve flattens beyond $|l| > 3^\circ$. The velocity dispersion profile remains higher than 75 km s $^{-1}$ even for the fields at $l = 10^\circ$. The M giants show both less rotation and greater velocity dispersion than do the bulge planetary nebulae of Beaulieu et al. (2000). The rarity of PNe and the difficulties of distance determination make them a more problematic population; we suspect many at large l are disk members.

In Figure 4, we compare the Zhao (1996) model in longitude-velocity space with our radial velocities, both sampling the slice at $b = -4^\circ$; we have smoothed the data in longitude by 0.5° and 8 km s $^{-1}$ in velocity. The region of the model bounded by the box at the lower right samples stochastic orbits. The region could contain retrograde orbits, which are lacking in the model (by construction). We can conclude that the addition of retrograde orbits to the model would help in resolving this discrepancy.

The comparison with the Zhao (1996) model and the data is revealing; the model is clearly rotating too fast but the fit to the velocity dispersion profile is excellent. It is interesting that the $(l, b) = (8, 7)$ K giant field of Minniti et al. (1992) agrees with our rotation curve (44.5 km s $^{-1}$); faster rotation (and a lower velocity dispersion) is observed in his $(l, b) = (12, 3)$ field that might be disk dominated. Menzies (1990) used Miras to sample velocities over a wide range in longitude. Small numbers, or disk population, might be invoked to explain the more rapid rotation observed for SiO masers (Izumiura et al. 1995). Our data are at odds with the widely held view that the bulge has solid body rotation. The relatively high velocity dispersions of our fields is reassuring in the sense that the M giant selection criterion is yielding good kinematic probes of the bulge/bar population.

Extending this survey to a larger number of fields in the bulge offers the possibility of undertaking detailed tests of dynamical models, something that is not presently possible in distant galaxy populations. This will give new insights into the structure and dynamics of the bulge, and into the formation of the Milky Way.

The authors acknowledge support from STScI grant GO-10816 and NSF grant AST-0709731. The authors are grateful to Jan Kleyna for helpful comments. This publication makes use of data products from the Two Micron All Sky Survey, which is a joint project of the University of Massachusetts and the Infrared Processing and Analysis Center/California Institute of Technology, funded by the National Aeronautics and Space Administration and the National Science Foundation.

Facilities: CTIO.

REFERENCES

- Alcock, C. et al. 2000, ApJ, 541, 734
 Babusiaux, C., & Gilmore, G. 2005, MNRAS, 358, 1309
 Beaulieu, S., Freeman, K.C., Kalnajs, & Saha, P. 2000, AJ, 120, 85
 Binney, J., Gerhard, O., & Spergel, D. 1997 MNRAS, 288, 36
 Blanco, V.M., McCarthy, M.F., & Blanco, B.M. 1984, AJ, 89, 636
 Blanco, V.M. 1987, AJ, 93, 321
 Blanco, V.M. 1988, AJ, 95, 1400
 Blanco, V.M. 2001, ARA&A, 39, 1
 Blum, R. D., Carr, J. S., Depoy, D. L., Sellgren, K., & Terndrup, D. M. 1994, ApJ, 422, 111
 Blum, R. D., Carr, J. S., Sellgren, K., & Terndrup, D. M. 1995, ApJ, 449, 623
 Dwek, E. et al. 1995 ApJ, 445, 716
 Frogel, J.A., & Whitford, A.E. 1987, ApJ, 320, 199
 Fulbright, J. P., McWilliam, A., & Rich, R. M. 2006, ApJ, 636, 821
 Han, C., & Gould, A. 2003, ApJ, 592, 172
 Izumiura, H., Deguchi, S., Hashimoto, O., Nakada, Y., Onaka, T., Ono, T., Ukita, N., & Yamamura, I. 1995, ApJ, 453, 837
 Kent, S.M. 1992, ApJ, 387, 181
 McWilliam, A., & Rich, R. M. 1994, ApJS, 91, 749
 Menzies, J. W. 1990, Workshop on Bulges of Galaxies, 115
 Minniti, D., White, S. D. M., Olszewski, E. W., & Hill, J. M. 1992, ApJ, 393, L47
 Minniti, D. 1996, ApJ, 459, 175
 Mould, J.R. 1983, AJ, 273, 530
 Rich, R. M. 1990, ApJ, 362, 604
 Rich, R. M., & Origlia, L. 2005, ApJ, 634, 1293
 Sadler, E., Rich, R.M., & Terndrup, D.M. 1996, AJ, 112, 171
 Schlegel, D. J., Finkbeiner, D. P., & Davis, M. 1998, ApJ, 500, 525
 Sahu, K. C. et al. 2006, Nature, 443, 534
 Sharples, R., Walker, A. & Cropper, M., 1990, MNRAS, 246, 54
 Skrutskie, M.F. et al. 2006, AJ, 131, 1163
 Stanek, K. Z., Udalski, A., Szymanski, M., Kaluzny, J., Kubiak, M., Mateo, M., & Krzeminski, W. 1997, ApJ, 477, 163
 Sumi, T. et al. 2004, MNRAS, 348, 1439
 Tyson, N.D., & Rich, R.M. 1991, ApJ, 367, 547
 Zhao, H.S. 1996, MNRAS, 283, 149

TABLE 1
OBSERVED BULGE ROTATION CURVE AND VELOCITY DISPERSION PROFILE

l (degrees)	b (degrees)	RA (J2000.0) (hh:mm:ss.s)	DEC J2000.0 ($^{\circ}$:':":')	N	v (km s $^{-1}$)	err(v) (km s $^{-1}$)	σ (km s $^{-1}$)	err(σ) (km s $^{-1}$)
-9.98	-3.99	17:36:31.47	-39:30:42.9	95	-53.9	8.2	80.0	5.8
-9.01	-4.00	17:39:10.83	-38:41:41.7	101	-28.1	7.7	77.0	5.4
-7.98	-4.00	17:41:56.69	-37:49:13.2	101	-36.3	7.9	79.6	5.6
-6.98	-3.99	17:44:33.22	-36:57:55.3	103	-54.8	8.5	85.8	6.0
-6.00	-3.99	17:47:03.54	-36:07:46.5	105	-36.3	8.5	86.8	6.0
-3.99	-3.98	17:52:02.74	-34:24:11.0	108	-43.9	9.2	96.0	6.5
-3.01	-3.99	17:54:26.79	-33:33:26.6	109	-39.9	10.7	111.5	7.6
-1.99	-3.98	17:56:50.87	-32:40:49.5	107	-18.2	10.1	104.4	7.1
-0.02	-3.99	18:01:28.27	-30:58:18.6	110	-8.3	10.7	112.2	7.6
-0.02	-3.99	18:01:28.27	-30:58:18.6	110	-13.4	10.7	112.2	7.6
1.04	-3.95	18:03:43.51	-30:01:49.9	72	4.7	13.0	110.2	9.2
2.00	-4.00	18:06:02.64	-29:13:17.4	107	36.1	11.2	115.5	7.9
3.99	-3.98	18:10:19.36	-27:28:32.3	105	35.7	10.2	105.0	7.2
6.01	-3.99	18:14:40.05	-25:42:06.9	108	56.0	8.5	87.8	6.0
6.99	-3.96	18:16:34.61	-24:49:41.9	104	36.5	9.2	94.0	6.5
7.99	-3.99	18:18:44.88	-23:57:51.7	107	50.6	8.5	87.9	6.0
9.01	-3.98	18:20:47.51	-23:03:31.1	101	27.0	7.4	74.3	5.2
10.00	-3.99	18:22:50.13	-22:11:12.6	106	41.7	8.2	83.9	5.8